Eurographics Workshop on Visual Computing for Biology and Medicine (2012)
T. Ropinski, A. Ynnerman, C. Botha, and J. B. T. M. Roerdink (Editors)

On the Value of Multi-Volume Visualization for Preoperative Planning of Cerebral AVM Surgery

F. Weiler[1], C. Rieder[1], C. A. David[2], C. Wald[2], and H. K. Hahn[1]

[1]Fraunhofer MEVIS, Bremen, Germany
[2]Lahey Clinic Medical Center, Burlington, MA, USA

Abstract

Surgical treatment of cerebral arteriovenous malformations (AVMs) requires thourough preoperative planning for the intervening neurosurgeon. The goal of such planning is to gain a precise understanding of the patho-anatomy of the malformation, specifically about the location and spatial relation of normal and abnormal structures. A key element in this process is the identication and localization of arteries feeding into the lesion, and veins draining it. In this paper, we demonstrate how state-of-the-art techniques from the field of computer graphics and image processing can support neurosurgeons with this task. We address the problem by merging multiple angiographic image sets within a 3D volume rendering pipeline. Datasets from clinical imaging studies were remotely processed at our institute, returned to the institution of origin, and finally visualized in an interactive application, allowing the neurosurgeon to explore the different images simultaneously. Here, we present three case studies along with the medical assessment of an experienced neurosurgeon.

Categories and Subject Descriptors (according to ACM CCS): I.3.6 [Computer Graphics]: Methodology and Techniques—Interaction techniques; I.3.8 [Computer Graphics]: Applications—; J.3 [Life And Medical Sciences]: Health—

1. Introduction

Arteriovenous malformations (AVM) of the brain are rare vascular disorders that are characterized by the presence of direct connections between arteries and veins. These form a kind of vascular short-circuit which is comprised of numerous coiled and convoluted connections, the nidus of the lesion. The nidus may be fed by one or more arteries, the feeders, and drains into one or more veins. To complicate things, additional "en passage" vessels may be involved, supplying both the AVM as well as important functional areas of the brain. Ligation of such feeders would cause postoperative neurological deficits and must therefore be avoided. Approximately 0.01 - 0.5% of the population are affected by cerebral AVMs.

Neurosurgical treatment of AVMs requires a precise understanding of the underlying angioarchitecture. It is crucial to identify all feeding arterial branches beside the draining veins. During surgery, the first step after locating the nidus is to ligate the main feeding arteries. Afterwards, the nidus can be dissected from the surrounding brain tissue before the draining veins can be ligated and the nidus removed. Failure to identify the feeders or ligation of the draining veins prior to obliteration of all feeders may cause rupture of the nidus, resulting in intraoperative hemorrhage and brain swelling, which may lead to serious patient impairment. Ligation of “en-passage" arteries would cause insufficient oxygen supply of connected parts of the brain accompanied by the risk of postoperative neurological deficits.

Considering these conditions, it becomes apparent that a complete understanding of the structure of the AVM prior to surgery is crucial for successful dissection. This, however, is a challenging task. First, there is no single imaging modality that could provide all required information about the neurovascular structures. Instead, a number of techniques exist that are capable of identifying individual parts of the relevant anatomy. Second, it is difficult to create a mental 3D model of the complex vascular configurations found in cerebral AVMs. At this point, the conventional 2D slicewise representation of tomographic images performs particularly poor

DOI: 10.2312/VCBM/VCBM12/049-056

in supporting the neurosurgeon with the generation of such a 3D model.

To overcome these difficulties, we have developed a visualization framework that allows for interactive exploration of multiple tomographic images in a 3D multi-volume rendering system. Images derived from multiple magnetic resonance imaging (MRI) sequences are combined and preprocessed in a semi-automatic manner. The resulting datasets can be visualized simultaneously using individual look-up tables and clipping planes per dataset. We utilize a volume renderer that implements a modular shader concept which allows for application of individual shading effects like illumination, clipping, or other custom effects per volume. Also, each volume can be of arbitrary voxel size and can be transformed by the renderer at runtime.

2. Imaging Background

The standard clinical imaging protocol used for AVM diagnostics comprises a combination of several tomographic and projection-based image acquisitions. The highest level of detail can be achieved with a digital subtraction angiography (DSA), in which a contrast agent is injected directly into the affected arterial branch through an endovascular catheter. During the inflow of contrast agent, X-ray projection images are acquired sequentially and subtracted from an initial reference image. This allows dynamic imaging of the distribution of the contrast agent through cerebral vasculature at very high spatial and temporal resolutions. Contrast-enhanced CT angiography (CTA) is a tomographic technique capable of generating high-resolution 3D images with voxel size in the order of $0.3mm^3$ and below. CTA of the head delivers high contrast of vascular structures. It is capable of displaying both the arterial and the venous tree with a high level of detail. Magnetic Resonance Imaging (MRI) provides a variety of different contrasts for displaying intracerebral structures. The primary MR imaging technique for this is time-of-flight (TOF) angiography, which allows to selectively visualize arteries or veins. An arterial TOF can be used to acquire images with a voxel size in the order of $0.5 - 1mm^3$, which allows visualizing relatively thin vessels compared to other MR-angiography sequences. With significantly lower spatial resolution, venous TOF images are most useful for displaying larger veins. Besides TOF MR-angiography, contrast-enhanced T_1-weighted imaging (CE-T_1) can also be used for displaying cerebral vessels.

3. Related Work

Multimodal visualization for neurosurgery planning has become a field of intense research in recent years. Beyer et al. [BHWB07] introduce methods for the visualization of multimodal data for neurosurgical planning. To remove the cranial bone, skull peeling is presented as an extension of the opacity peeling algorithm introduced by Rezk-Salama et al. [RSK06] using registered CT and MRI data. In [JBB*08], methods for illustrative visualization of fMRI data combined with anatomy of the brain are presented. Rößler et al. [RTF*06] describe a multi-volume framework for the visualization of functional brain images using the graphics hardware to allow interactive visual exploration of the data. Interactive visualization techniques for combining multimodal datasets, such as functional data, are discussed in [BBM*07] to assist neurosurgical planning. Köhn et al. present in [KWK*07] an application for neurosurgical planning and assessing of risk structures. In their work, they visualize vessels as well as functional data such as fMRI activation areas and fiber tracts from DTI. Rieder et al. present a prototype for visualization of multimodal data for neurosurgical tumor treatment [RRRP08]. They describe methods to enhance important functional data and visualize these data combined with anatomical data along a virtual access path. [RSHP08] addressess the issue that fused multimodal visualizations typically complicate the recognition of anatomical details of the brain and pathological tissue at the same time without loss of information. Furthermore, in the volume rendering, important structures as well as suspicious high-intensity signals from multiple sequences are enhanced using a fuzzy clustering approach.

Interactive clipping techniques are powerful and general utilities for the visualization of volume data [WEE02, WEE03]. Manssour et al. [MFOF02] verify that cutting tools can reveal additional diagnostic information for multimodal volume rendering. Wu et al. [WAR] present fast parallel slice cutting and partial exposing algorithms which are used for real-time volume rendering to support image-guided surgery and therapy planning. Tappenbeck et al. [TPD] present distance as a second dimension for transfer function definition. They compute a distance volume by slice-based selection of distance ranges. Zhou et al. [ZHT02] present focal region-guided enhancement of features in the volume rendering. In [ZDT], the proposed method is extended by a distance measure as the main factor to control the volume features in the context region.

In the field of intracranial aneurysm visualization, Higuera et al. [HST*03] make use of a 2D transfer functions based on measured values and gradient magnitudes extracted from the CTA data to enhance the 3D visualization of intracranial aneurysms. Nishihara et al. [NT01] report in a clinical study the usefulness of volume-rendered visualizations using computed tomographic angiography for surgical planning of aneurysms. Bullit et al. [BAB*01] use vessel trees to visualize the relationship to the lesion in three dimensions. The proposed methods include information about the hierarchical vasculature to allow color coding and interactive occlusion of subtrees. Furthermore, visualization results from two AVM cases are compared with findings during surgery.

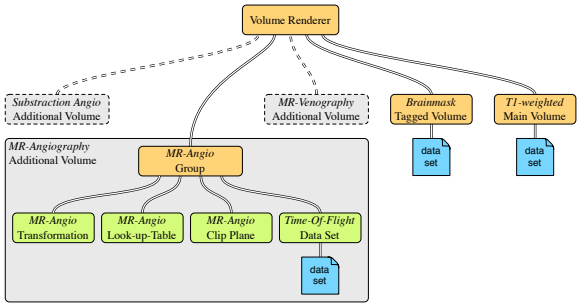

Figure 1: *Illustrative description of the multi-volume rendering scene graph. Every additional volume has corresponding child nodes for clipping, transfer function and the volume texture.*

4. Methods

The underlying idea of our approach is to allow simultaneous volumetric renderings of the various different datasets available for a case and to provide the neurosurgeon with an efficient way to combine and integrate the information obtained from the individual datasets, without the difficulty of performing a mental fusion of the complex and partly redundant information. This is achieved by presenting different datasets simultaneously using direct volume rendering in combination with a selection of tools to interactively compose these datasets to a meaningful visualization. We avoid using image segmentation to directly reconstruct vascular trees in favor of presenting the datasets in a mostly unmodified manner, thereby avoiding the risk of discarding information from the images. Thus, the final interpretation of structures visible within each image lies within the responsibility of the medical user.

4.1. Data preprocessing

Our visualization framework requires datasets to pass through a preprocessing pipeline, prior to being suited for volume rendering. Necessary preprocessing steps include registration of the multiple images into a common coordinate system, segmentation of the brain from native T_1-weighted images, and an enhancement step of both the CE-T_1 as well as the TOF images. Since the quality of the preprocessing results is crucial for the clinical review of the data, we chose to implement a supervised semi-automatic approach for brain segmentation and image registration. The workup for each case can be performed by a medical assistant and requires at most 10 minutes for a trained user. All additional processing steps are calculated fully automatic. The final preprocessing results are saved and can be imported into the viewer application within several seconds. See [WRD*11] for further details on the preprocessing pipeline applied.

4.2. Shaded Multi-Volume Rendering

Direct multi-volume rendering is used to visualize the three-dimensional shape of the AVM and the surrounding angioarchitecture to support the neurosurgeon in surgery planning. Technically, we utilize a multi-volume rendering framework which uses a scene-graph to dynamically compose and compile a GLSL shader. Multiple datasets can be added to the scene-graph at run-time. Corresponding shading parameters, clip planes and transfer functions are independently defined for each data set and can be manipulated interactively by the user.

For the task of analyzing AVM cases, the typically provided images comprise a T_1-weighted main volume, an MR subtraction angiography and both an arterial and a venous time-of-flight dataset. Each dataset can be independently classified with a separate transfer function using windowing by the medical expert. Spatial alignment of the different images is performed within the volume renderer, taking benefit from the fast transformation and interpolation capabilities provided by the GPU. For that, each additional dataset with its corresponding transformation matrix is loaded into our volume renderer and the transformation is applied per fragment on the graphics hardware.

To visually distinguish the brain from the skull, a brain mask is calculated in the preprocessing stage that is then used to classify voxels of the T_1-weighted main volume as either brain or skull, with an individual transfer function being applied to each. To visually enhance perception of grey- and white-matter tissue, the transfer function for the brain is automatically derived from the histogram of the brain using a fit of a multi-Gaussian mixture model [HJL*04]. Volume shading is utilized for all datasets in our visualization to enhance depth perception. Therefore corresponding gradients are calculated and stored in an addition texture for every data set. In the shader program, the gradient textures are used to calculate Phong shading individually for each data set.

Figure 1 gives a schematic overview of the structure of the volume renderer. See [RPLH11] for an in depth explanation of the technical details of the multi-volume rendering technique implemented.

4.3. Independent Clip Planes

When simultaneously rendering multiple overlapping images, one has to deal with the problem of occlusion. Various non-transparent anatomical structures may overlay other important structures, e.g. intracranial vessels are mostly occluded by surrounding brain tissue. To allow for exploration of these interior vascular structures, individual clip planes are used for each volume. To keep interaction with the multiple clip-planes simple, we define a master clip-plane to which all others are aligned in parallel, with individual offsets each. The orientation of the master clip-plane is controlled from the 2d-viewer. To allow for consistent volume

shading on the clip-planes, we use the inverted plane normals as gradients at the clip plane's boundary [WEE03]. Hence, the neurosurgeon is able to easily cut away skull and brain while keeping the vessels visible.

4.4. Focus Of Attention

An additional approach to dealing with the occlusion problem is to attenuate structures depending on their distance to a given point of interest. Because clip planes are commonly defined in three axis aligned directions, they are not well suited for attenuation of arbitrarily shaped structures such as unimportant vessels. To overcome this issue, we utilize a focus of attention, which defines a spherical area of interest around a given point. Then, the distance between every voxel and the focus point is calculated in a shader. The resulting distance is used to manipulate the color saturation and alpha value using a customizable distance measure [RRRP08]. This technique has proven particularly useful for analyzing AVM images, as it allows to put a focus on the lesion, analyze in detail the vessels surrounding it, and attenuating the large number of distant vessels that would otherwise distract the viewer.

4.5. Overall implementation

Our system has been implemented as a standalone medical software assistant, that runs on conventional PC or Mac hardware with a current generation GPU processor. The preprocessed datasets are loaded and analysis of a case can be done without any further manual processing. Cross-sectional slice views in the three standard planar reformations can be used to navigate through the datasets, to control the position and alignment of the primary clipping plane, and also to define the position of a focus of attention. A panel on the right gives access to all control elements required for interaction. The centrally located main viewer of the application is reserved for the volume rendering of the data.

5. Results and Discussion

The software has been installed in the radiology department of our clinical partner, where it has been used to retrospectively analyze three AVM cases that have undergone surgery during the years 2008 to 2010. Analysis of these cases was done by the same neurosurgeon who had performed the actual neurosurgical procedures. In the following section, the potential usefulness of our application for preoperative planning is discussed by summarizing the findings based on our tool, accompanied with documentations of how they correlate with intraoperative findings.

5.1. Case 1

The first case consists of a AVM classified as Spetzler Martin Grade III [SM86], located in the frontal opercular regions on the dominant hemisphere. The main surgical challenges in this case relate to speech and motor function of the brain as well as the anatomical location and the visualization of the AVM. The following surgical issues were specified by the neurosurgeon:

- Opening the Sylvian fissure in order to visualize the surface representation of the AVM and identify the main feeders, isolating and disconnecting them.
- Identification of feeders that are “en passage". This is critical in this location, as disrupting a vessel that is merely supplying branches to the AVM but continuing on to supply critical motor or speech regions would result in poor neurological outcome.
- Following the main venous drainage to the AVM nidus and then dissecting the AVM away from the surrounding brain without injuring the adjacent eloquent cortex.

The visualization application provided a critical understanding of the precise location of the AVM. MR-Angiography and MR-Venography datasets were used for the identification of the venous drainage pattern and the exact location of the feeding vessels. The focus of attention proved helpful to reduce visual clutter of unaffected vessels. Furthermore, the topography of the feeding arteries in relation to the venous drainage and cortical anatomy was visualized using the clip plane technique. Essentially, the visualization allowed the surgeon to visualize exactly what he encountered during surgery, along with the location of the feeders, and most importantly, identification of an “en passage" vessel.

Figure 2 (a) shows an annotated overview visualization of Case 1. The clip plane is applied to the brain, allowing a clear view of the Sylvian fissure and the underlying feeding vessel at the brain's surface. Furthermore, the draining vein and its pathway are clearly visible in the volume rendering. In Figure 2 (b), a detailed view of the nidus is presented, with an activated focus of attention and the brain and the skull completely clipped away. The focus is set to the AVM center, resulting in the attenuation of unimportant vascular structures and hereby enhancing the nidus. Following the path of the feeding arteries, the spatial location of the “en passage” vessel can be recognized in the center of the lesion.

In this particular case, the volume visualization would have been invaluable for surgery planning. It allowed to visualize what to expect without the need for “mental gymnastics” when trying to fuse all the 2D data mentally. During surgery, the neurosurgeon would have been able to correlate the vessel that he thought was the “en passage" with the volume rendering and follow its course, sealing the branches to the AVM and preserving the main vessel. Also, understanding the topography of the lesion would have been significantly simplified, allowing to explore precisely the gliotic plane which is important to avoid straying into the normal adjacent cortex and white matter.

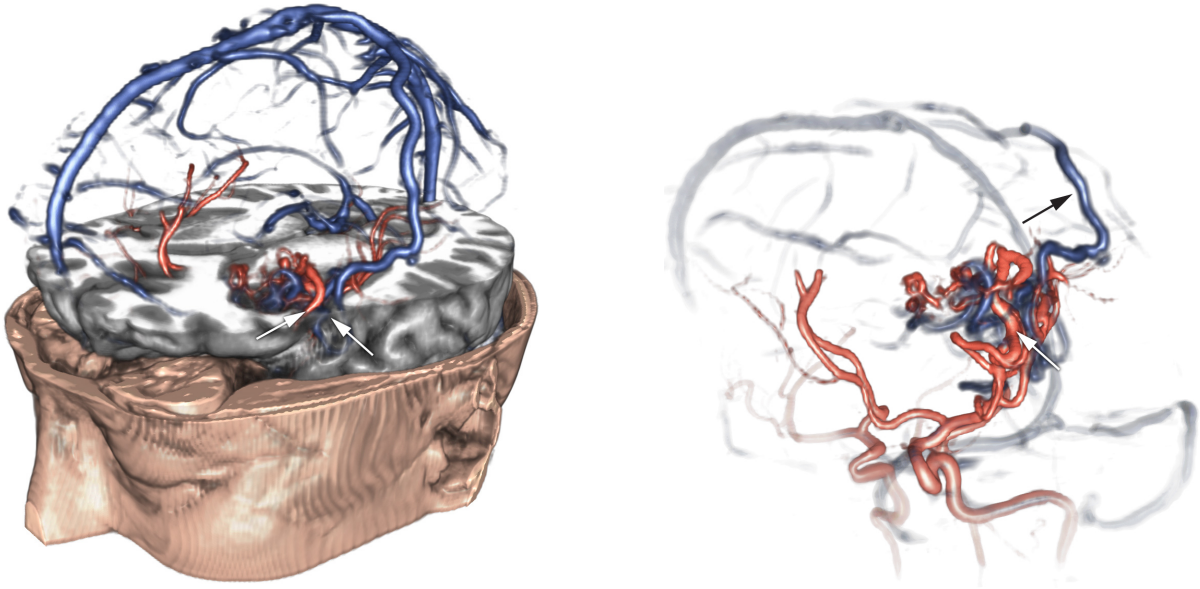

(a) (b)

Figure 2: *(a) Volume visualization of Case 1 using T1, MR-Venograpy and MR-Angigrapy datasets. Utilizing the cut planes, the Sylvian fissure (right arrow) as well as an underlying arterial feeder (left arrow) can be illustrated. (b) Detailed rendering of Case 1. The AVM nidus is enhanced using the focus of attention technique. Arterious feeders (white arrow) and draining veins (black arrow) are visible in the vicinity of the AVM.*

5.2. Case 2

The AVM in this case is less complex and risky than the AVM of case 1. It is a Grade II AVM located in the insula of the right hemisphere. Again, the main challenges relate to motor function due to middle cerebral artery branch involvement. The AVM is located deep in the Sylvian fissure and has no obvious surface representation. One would need to open the Sylvian fissure to identify the AVM within a myriad of middle cerebral artery (MCA) branches and venous tributaries. Surgical issues include:

- Opening the fissure while dealing with arterialized veins. Several veins formed a network which would not allow complete opening without closing of a branch. In such cases, it is critical to know which branch could be taken safely. Taking the wrong one would result in immediate venous hypertension, brain swelling, and hemorrhage.
- Once the fissure is opened, following the main vein to the AVM was undertaken. However, due to the multitude of overlapping MCA branches, it is difficult to determine which are the true feeders, the “en passage" vessels and simply uninvolved MCA branches in the fissure.
- Once feeders are secured, resecting the AVM without straying into the deep white matter is important in this case, as the AVM extends into the claustrum and extreme capsule; delving too deep in this location could damage the internal capsule and result in hemiparesis or plegia.

For this case, the volume rendering allowed the neurosurgeon to gain an understanding of most of the topography and representation of the AVM as it relates to the insula and frontotemporal-Sylvian regions prior to opening the fissure. He was virtually able to determine which vein could have been sacrificed to open the fissure. The visualization clearly revealed that the main two feeders were straddling the main draining vein, allowing confirmation and isolation of these two vessels. One difficulty was determining the course of the MCA branch that was “en passage". The rendering gave the impression that a superiorly located vessel extending beyond the AVM was an “en passage" MCA branch when in fact, during surgery, it was a draining vein on the brain surface. This has been caused by the fact, that this particular vessel is enhanced in both, the TOF-angiography as well as the MRV. A more extensive exploration of the multiple datasets by modification of the individual transfer functions, finally helped to confirm the venous nature of this vessel.

Figure 3 (a) shows the volume rendering of Case 2. The brain is clipped away so that the AVM can be located deep within the Sylvian fissure (white arrow). MR-Angiography and MR-Venography datasets are used to visualize the feeding arteries and the draining veins. The posterior draining vessel (black arrow) is visible in both datasets which confused the neurosurgeon. In Figure 3 (b), a close-up volume rendering of the AVM nidus is presented. Using the focus of

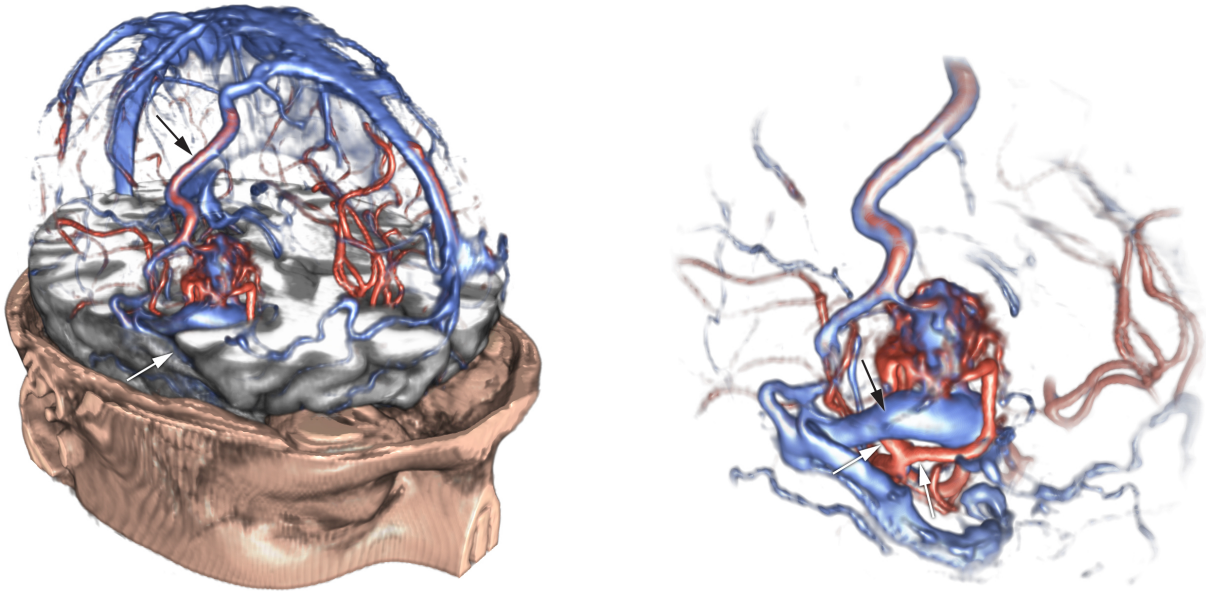

(a) (b)

Figure 3: *Volume rendering of Case 2 using MR-Angiography and subtraction angiography. Figure (a) gives an overview of the case along with an anatomical reference. The AVM is located deep in the Sylvian fissure (white arrow). The presence of the draining vein (black arrow) in both datasets confused the neurosurgeon in identifying the vessel. Figure (b) gives a detailed visualization of the AVM. The main two feeders (white arrows) straddle the main draining vein (black arrow).*

attention, the neurosurgeon has a clear view to explore and understand the shape of the arterial feeders and the draining vessels in detail. The main two feeders (white arrows) straddle the main draining vein (black arrow).

5.3. Case 3

The AVM of case 3 is a rather small grade II AVM of relatively low risk. The only significant risk and challenge is its location in the sensory strip and proximity to the motor cortex. This leads to an increased risk of postoperative lower extremity paralysis or paresis. Furthermore, the AVM is located deeply inside a sulcus so there would be no surface representation other than the draining vein. Understanding the topography and relation to the motor strip is critical in this case.

Here, the visualization allowed the neurosurgeon to visualize the sulci and general topography of the region without the need for imprecise mental fusing of the MRI and conventional CT-Angiography. This allowed him to explore the draining vein leading to the sulci. This would have helped determining the appropriate sulci to open and follow it in. Once identified, the feeding vessels were clear, and the volume rendering was of no additional value in that aspect. However, one difficulty found with the visualization was precisely estimating the extent of the nidus using the viewer application. It appeared that the volume rendering underestimated the size of the AVM nidus in this case. It was difficult to visualize the exact extent of the nidus on the model. If one followed the main vein on the rendering, the AVM became apparent, but its full extent and borders were not clearly visualized. This issue is likely due to both, the small size of the AVM and relatively low image resolution of the time-of-flight datasets, particularly the MR-Venography.

Figure 4 (a) shows the volume rendering of Case 3. A clip plane is set on top of the AVMs location in order to visualize the draining veins (black arrows) with respect to the gyri and sulci of the brain. Furthermore, a feeding artery following the brain's surface to the AVM is visible (white arrow). In (b), the brain is completely clipped away and the focus is set to the AVM's nidus. The image shows an additional feeding artery passing through the brain as well as the draining veins at the brain's surface. In comparison to our visualization, a conventional maximum intensity projection (MIP) of the MRV is shown in (c). Although the same vascular structures are present in both renderings, it is significantly more difficult to grasp the vascular configuration of the lesion from this conventional presentation.

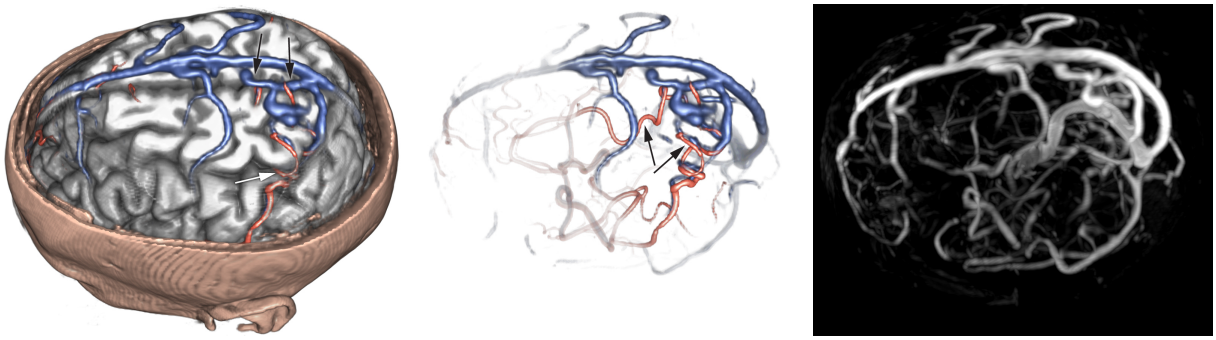

(a) (b) (c)

Figure 4: *Volume rendering of Case 3. In (a), the location of the draining veins (black arows) can be explored, incorporating the brain's anatomy. Image (b) shows the feeding arteries (black arrows) and the draining veins. In (c), a conventional MIP rendering of the MR-Venography is presented.*

5.4. Discussion

In contrast to the traditional MIP rendering of vascular structures, our volume visualization allows visualizing fused anatomical structures such as the gyri and sulci simultaneously with various additional vascular datasets. This multimodal visualization allows a neurosurgeon to understand the three-dimensional anatomy of the AVM nidus. Moreover, the extent and spatial position of the lesion can be estimated with respect to the brain's anatomy. For instance, the evaluation of the lesion's relation to eloquent areas is of high importance for surgery planning. Furthermore, feeding arteries and draining veins can be identified utilizing the combined rendering of MR-Venography with time-of-flight MR-Angiography datasets. In contrast, with a traditional MIP rendering of such datasets the neurosurgeon has to mentally fuse varying visualizations of the vascular structures, which is challenging, particularly if a complex angioarchitecture is present. Also, identification of "en-passage" vessels is critical during surgery planning, because disruption of a vessel that is merely supplying branches to the AVM but continuing on to supply critical motor or speech regions would result in poor surgery outcome (cf. Case 1 and Case 2).

A potential drawback of our method is caused by the circumstance that partially ambiguous presentation of parts of the vascular tree in arterial and venous images could potentially lead to misinterpretation of the data. This, however, rather relates to the image acquisition technique as opposed to the visualization technique applied. It needs to be addressed by making careful exploration of all available datasets mandatory during planning, in order to specify the precise nature of the vessels surrounding the AVM nidus (cf. the feeding vein in Case 2). Another aspect relating to the necessity for careful data exploration is the fact that depending on the window settings of transfer function of a dataset in combination with the limited image resolution, small vessels could possibly become invisible in the volume rendering and thus not be considered for surgical planning. More critically, the impression of the lesions size will also depend on the settings of the transfer function, causing a potential risk of underestimating the lesion's true extent. The latter points underline the requirement for careful exploration of all datasets, which needs to assured by the neurosurgeon performing the preoperative planning.

6. Conclusions

In this work, we have presented a data-processing pipeline along with an interactive volume-rendering framework for visualization of cerebral vascular structures based on multiple MRI datasets. Development has been primarily motivated by the clinical challenge posed to neurosurgeons during the preoperative analysis and risk assessment of AVMs. Specifically, this challenge is defined by the difficulty of understanding the complex angioarchitecture of the AVM. Also, understanding the spatial relation of the nidus to eloquent ares of the brain, which strongly affects the possible access path to the lesion may be a difficult task in certain cases. Exclusively relying on conventional 2D slice representations of tomographic images results in a complicated mental process of generating a 3D model of the lesion.

We addressed this problem by combining multiple MR-based angiographic datasets within a multivolume rendering framework that allows individual shading and clipping for each volume. Vascular trees are presented without performing an explicit segmentation in order to avoid the risk of hiding information from the data caused by insufficiently accurate segmentation results. Instead, our approach allows the neurosurgeon to explore the given vascular anatomy interactively, allowing him to fuse his prior knowledge with patient-individual findings from the available images. The possibility of manipulating individual transfer functions of

each dataset especially facilitates the mental classification of affected vessels as either arterial or venous. We have demonstrated the usefulness of this technique by discussing results from three clinical case studies. These cases were re-analyzed retrospectively using the method described in this paper. The performing neurosurgeon repeatedly stated how much the possibilities of the 3D visualization would have helped him plan and perform the resection. For selected cases, he rated the visualizations as invaluable, emphasizing that he would not want to miss such techniques in the future.

Our future work will focus on two aspects. First, we would like to incorporate CTA images in our visualizations, which currently achieve the highest level of detail of cerbrovascular structures. To do so, the occlusion problem of the skull bone needs to be addressed, for which a simple masking with a brain segmentation typically does not yield satisfying results. Second, and more importantly, we would like to exploit the fact that the combination of multiple angiographic datasets creates a redundancy within the data that could be explored to improve the classification of vessels into arterial or venous branches. Such a technique could further reduce the potential danger of misinterpreting the role of individual vessels.

Acknowledgments

The authors wish to thank Christiane Engel for assisting with the preparation of case data for our evaluation. Data used in this article are courtesy of Lahey Clinic Medical Center, 41 Mall Road, Burlington, MA 01805.

References

[BAB*01] BULLITT E., AYLWARD S., BERNARD E., GERIG G., WOMACK B.: Computer-Assisted Visualization of Arteriovenous Malformations on the Home PC. *Neurosurgery 48*, 3 (2001), 576 – 583. 2

[BBM*07] BLAAS J., BOTHA C., MAJOIE C., NEDERVEEN A., VOS F.: Interactive visualization of fused fmri and dti for planning brain tumor resections. *Proceedings of SPIE* (Jan 2007). 2

[BHWB07] BEYER J., HADWIGER M., WOLFSBERGER S., BÜHLER K.: High-Quality Multimodal Volume Rendering for Preoperative Planning of Neurosurgical Interventions. *Visualization and Computer Graphics, IEEE Transactions on 13*, 6 (2007), 1696–1703. 2

[HJL*04] HAHN H. K., JOLLY B., LEE M., KRASTEL D., REXILIUS J., DREXL J., SCHLÜTER M., TERWEY B., PEITGEN H.-O.: How accurate is brain volumetry? a methodological evaluation. In *MICCAI – Medical Image Computing and Computer-Assisted Intervention* (Berlin, 2004), Barillot C., Haynor D., Hellier P., (Eds.), vol. 3216, Springer, pp. 335–342. 3

[HST*03] HIGUERA F., SAUBER N., TOMANDL B., NIMSKY C., GREINER G., HASTREITER P.: Enhanced 3d-visualization of intracranial aneurysms involving the skull base. *Medical Image Computing And Computer-Assisted Intervention - Miccai 2879* (Jan 2003), 256–263. 2

[JBB*08] JAINEK W. M., BORN S., BARTZ D., STRASSER W., FISCHER J.: Illustrative hybrid visualization and exploration of anatomical and functional brain data. *Comput Graph Forum 27*, 3 (Jan 2008), 855–862. 2

[KWK*07] KÖHN A., WEILER F., KLEIN J., KONRAD O., HAHN H. K., PEITGEN H.-O.: State-of-the-Art Computer Graphics in Neurosurgical Planning and Risk Assessment. *Eurographics Short Papers and Medical Prize Awards* (2007), 117–120. 2

[MFOF02] MANSSOUR I., FURUIE S., OLABARRIAGA S., FREITAS C.: Visualizing inner structures in multimodal volume data. *Computer Graphics and Image Processing, 2002. Proceedings. XV Brazilian Symposium on* (2002), 51–58. 2

[NT01] NISHIHARA M., TAMAKI N.: Usefulness of volume-rendered three-dimensional computed tomographic angiography for surgical planning in treating unruptured paraclinoid internal carotid artery aneurysms. *Kobe J Med Sci 47*, 5 (Oct 2001), 221–30. 2

[RPLH11] RIEDER C., PALMER S., LINK F., HAHN H. K.: A shader framework for rapid prototyping of gpu-based volume rendering. *Computer Graphics Forum 30*, 3 (2011), 1031–1040. 3

[RRRP08] RIEDER C., RITTER F., RASPE M., PEITGEN H.-O.: Interactive visualization of multimodal volume data for neurosurgical tumor treatment. *Computer Graphics Forum 27*, 3 (Jan 2008), 1055–1062. 2, 4

[RSHP08] RIEDER C., SCHWIER M., HAHN H. K., PEITGEN H.-O.: High-Quality Multimodal Volume Visualization of Intracerebral Pathological Tissue. In *Eurographics Workshop on Visual Computing for Biomedicine* (2008), pp. 167–176. 2

[RSK06] REZK-SALAMA C., KOLB A.: Opacity peeling for direct volume rendering. *Comput Graph Forum 25*, 3 (Jan 2006), 597–606. 2

[RTF*06] RÖSSLER F., TEJADA E., FANGMEIER T., ERTL T., KNAUFF M.: GPU-based Multi-Volume Rendering for the Visualization of Functional Brain Images. *Proceedings of SimVis* (2006), 305–318. 2

[SM86] SPETZLER R. F., MARTIN N. A.: A proposed grading system for arteriovenous malformations. *Journal of Neurosurgery 65*, 4 (1986), 476 – 483. 4

[TPD] TAPPENBECK A., PREIM B., DICKEN V.: Distance-based transfer function design: Specification Methods and Applications. *SimVis 2006*, 259–274. 2

[WAR] WU L., AMIN V., RYKEN T.:. *Proceedings of SPIE*, 61412R. 2

[WEE02] WEISKOPF D., ENGEL K., ERTL T.: Volume Clipping via Per-Fragment Operations in Texture-Based Volume Visualization. *Visualization, 2002. VIS 2002. IEEE* (2002), 93–100. 2

[WEE03] WEISKOPF D., ENGEL K., ERTL T.: Interactive Clipping Techniques for Texture-Based Volume Visualization and Volume Shading. *Visualization and Computer Graphics, IEEE Transactions on 9*, 3 (2003), 298– 312. 2, 4

[WRD*11] WEILER F., RIEDER C., DAVID C. A., WALD C., HAHN H. K.: AVM-Explorer: Multi-Volume Visualization of Vascular Structures for Planning of Cerebral AVM Surgery. *EG 2011 - Dirk Bartz Prize* (2011), 9–12. 3

[ZDT] ZHOU J., DORING A., TONNIES K.:. *Bildverarbeitung für die Medizin 2004: Algorithmen*, 199–203. 2

[ZHT02] ZHOU J., HINZ M., TONNIES K.: Focal region-guided feature-based volume rendering. *3D Data Processing Visualization and Transmission, 2002. Proceedings. First International Symposium on* (2002), 87– 90. 2